

Seismotectonic evaluation of off Nicobar earthquake swarms, Andaman Sea

**Karanam Kattil Aswini^{1,2}, Kattoju Achuta Kamesh Raju^{1,3*}, Pawan Dewangan¹,
Vadakkeyakath Yatheesh¹, Pabitra Singha¹, Telluri Ramakrushana Reddy¹**

¹CSIR-National Institute of Oceanography, Dona Paula, Goa 403004, India

²School of Earth, Ocean and Atmospheric Sciences, Goa University,
Taleigao Plateau, Goa 403206, India

³National Centre for Polar and Ocean Research, Ministry of Earth Sciences,
Vasco-da-Gama, Goa 403804, India

*Corresponding author. E-mail: kameshraj@gmail.com, kamesh@ncpor.res.in

Abstract

The Andaman Sea has experienced a number of earthquake swarms as a result of complex tectonics arising from oblique subduction, active volcanic arc, the backarc spreading center, and sliver fault systems. One of the most energetic offshore earthquake swarms occurred in the off Nicobar region of the Andaman Sea in January 2005, following the 26th December 2004 (9.1 M_w) Sumatra megathrust event. After a brief quiescence, this region got reactivated again after the 21st March 2014 (6.5 M_w) event, followed by the occurrence of earthquake swarms in March 2014, October 2014, November 2015, and April 2019. In the present study, we analysed the temporal variation of the b-value of these swarms using the global network data and the Ocean Bottom Seismometer data to understand their genesis. Temporal variation of b-value suggests that b-values are larger than unity for earthquake swarms, indicating volcanic origin. Bimodal distribution of frequency magnitude relation suggests that the earthquake swarms have occurred due to complex seismic processes controlled by both tectonic and volcanic activities. We propose that a combination of magmatic pulsation in the arc volcanism in response to 2004 and 2005 megathrust events and the 6.5 M_w magnitude 21st March 2014 event in off Nicobar region, and reactivation of sliver fault systems, are the dominant mechanisms for the observed frequent earthquake swarms.

Keywords: submarine arc volcanism, sliver strike-slip faults, earthquake swarms, Gutenberg-Richer relation and b-value, subsurface magma.

1. Introduction

Active submarine volcanoes constitute one of the major structural elements of the convergent plate boundaries, and such volcanoes along with associated earthquake swarms are potential geohazards. The long-term monitoring of submarine volcanic activity and direct evidence of surface and subsurface magma movements are often difficult in the oceanic environment, and hence, are less studied as compared to onshore volcanoes. One of the effective tools to monitor the activity of submarine volcanoes is earthquake seismology. There exists a strong correlation between volcanic eruptions and volcano-tectonic earthquake swarms (Hill, 1977). Volcanic eruptions may be triggered from distant or local major earthquakes (Linde and Sacks, 1998), especially in subduction zones, where megathrust earthquakes can induce volumetric decompression leading to enhanced backarc volcanic activity (Walter and Amelung, 2007). Several studies suggested that earthquake swarms occur due to stress perturbation associated with fluid migration in a magmatic or hydrothermal system through new or recently formed crustal heterogeneities such as fissures and cracks (Hill, 1977; Toda et al., 2002). Earthquake swarms observed in the active volcanoes such as Usu Volcano and Kirishima volcano in Japan (Zobin et al., 2005; Chiba and Shimizu, 2018), Yellowstone volcanic field in the United States (Farrell et al., 2009; Farrell et al., 2010), Fogo Volcano and Congro Volcanic Fissural System at Azores archipelago (Silva et al., 2015), Quito swarm of Guagua Pichincha volcano (Legrand et al., 2004) are some of the examples that show a direct relationship between earthquake swarms and volcanic activity. Gutenberg-Richter magnitude relationship (parameterized by b-value) is an effective method to differentiate earthquakes in terms of tectonic or volcanic activity (Frohlich and Davis, 1993; Wiemer and Wyss, 1997; McNutt, 2004). Generally, low b-values ($<$ less than unity) suggest tectonic domain (Frohlich and Davis, 1993), and larger values (>1 to 3) suggest volcanic activity (Wyss et al., 2001; McNutt, 2004).

Andaman Sea witnessed frequent and significant earthquake swarms after 26th December 2004 and 28th March 2005 megathrust events. The distinct and divergent rupture pattern of these megathrust events altered the volcano-tectonic activity and seismicity of the region (Lay et al., 2005; Singh, 2005; Gahalaut et al., 2006; Kamesh Raju et al., 2007). Subsequent to the December 2004 megathrust event, an energetic swarm occurred in January 2005 near the triple junction of ANF, West Andaman Fault (WAF), and Seulimeum Fault (SF). This swarm is closest to the 2004 earthquake rupture zone that experienced maximum co-seismic slip (Gahalaut et al., 2006, Banerjee et al., 2007, Kundu et al., 2012). The stress changes due to megathrust events, the tectonic elements such as sliver fault systems (GSF and ANF), and volcanism off Nicobar region have led to the most energetic 2005 swarm (Gahalaut et al., 2006; Banerjee et al., 2007; Gahalaut et al., 2008; Kamesh

Raju et al., 2012; Kundu et al., 2012). The off Nicobar region has experienced 4 distinct earthquake swarms in March 2014, October 2014, November 2015, and April 2019. The increase in the rate of occurrence of earthquake swarms after the 2014 M_w 6.5 event is intriguing. In the present study, we computed temporal variability of b-values to understand the genesis of earthquake swarms in the off Nicobar region.

2. Geodynamic Setting

Andaman-Nicobar-Sumatra subduction zone is an active oblique subduction zone in the northeast Indian Ocean. Indo-Australian plate subducts beneath the Burmese microplate resulting in the formation of a major island arc-trench system. The major tectonic elements consist of the subduction zone, sliver strike-slip faults (includes Great Sumatra Fault, Andaman Nicobar Fault, Andaman transform fault, Sagaing Faults), volcanic arc, and backarc basins (Kamesh Raju et al., 2004; Curray, 2005; Cochran, 2010). The volcanic arc extends from dormant Narcondam Island volcano, active Barren Island volcano to volcanic seamounts near Andaman backarc spreading center (ABSC), to submarine volcanoes near the Nicobar Islands, and joins the onshore volcanoes of Sumatra (Kamesh Raju et al., 2004; Curray, 2005) along the GSF. The GSF is a ~ 1900 km tectonic feature that accounts for the dextral strike-slip component of oblique convergence of Indo-Australian plate beneath Southeast Asian plate (Sieh and Natawidjaja, 2000). The northern segment of the GSF in the Andaman Sea bifurcated into Aceh Fault (AF) and Seulimeum Fault (SF) (Fig. 1). The proximity of the volcanic arc and the offshore extension of the GSF suggest that these major structural elements influence each other (Ghosal et al., 2012; Singh et al., 2013). The SF is an active fault while the AF has remained dormant for the past 100 ka (Sieh and Natawidjaja, 2000).

The region has witnessed two megathrust events on 26th December 2004 (Sumatra event M_w 9.0) and on 28th March 2005 (Nias event M_w 8.6), which have immensely impacted the seismicity of the region. The total rupture length and coseismic displacement of 2004 and 2005 events are 1700 km and 25 m, respectively (Lay et al., 2005; Fujii and Satake, 2007; Rhie et al., 2007). The maximum coseismic slip was nearly 20 m off NW Sumatra (Ammon et al., 2005; Singh, 2005; Subarya et al., 2006; Sieh et al., 2008; Singh et al., 2008; Singh et al., 2012). The megathrust events imparted static Coulomb stress along the major sliver fault systems, inhibited failure along the Sagaing Fault, and promoted failure along the Andaman Backarc Spreading Center (ABSC), Andaman-Nicobar Fault (ANF), and the Great Sumatra Fault (GSF) systems (Gahalaut et al., 2008; Cattin et al., 2009; Kundu et al., 2012). The January 2005 off Nicobar earthquake swarm has imparted additional Coulomb stress of almost 20 bar in the northern segment of the GSF (Cattin et al., 2009). The high Coulomb stress and the absence of high intensity earthquakes in the last 170 years along the offshore extension

of GSF (Bellier et al., 1997; Sieh and Natawidjaja, 2000) make this region prone to a high seismic hazard (Cattin et al., 2009).

3. Data and Methods

The study area is in the off Nicobar region between 6° N to 9° N and 93° E to 96° E covering the northern extent of GSF and submarine volcanoes. To understand the seismotectonics of the recent earthquake swarms in the region, we compiled earthquake data for a period of 20 years from 2000 to 2020 using IRIS and ISC catalogues and local network earthquake data. We used the ISC-EHB bulletin, which contains improved earthquake locations following the EHB algorithm (Engdahl et al., 1998). We also used Ocean Bottom Seismometer data (Dewangan et al., 2018; Singha et al., 2019), ISLAND station data (Srijayanthi et al., 2012), and IRIS data collected during 21st and 22nd March 2014. We identified 141 high-frequency earthquakes during 21st and 22nd March 2014 as detected by three or more OBS stations. We removed the overlapping events from different catalogues and made a single data file. The compiled data from all the sources yielded 2552 earthquake events in the off Nicobar region. The magnitude of earthquakes ranges from 2 to 6.5 on body wave magnitude (m_b) scale. We have converted the local magnitude (M_L) of earthquakes detected by OBS and ISLAND data to body-wave magnitude (m_b) using the conversion formula ($M_L = 0.802m_b + 0.3683$) obtained by the regression analysis. We have separated five energetic swarms that occurred in January 2005 (917 events), March 2014 (141 events), October 2014 (262 events), November 2015 (112 events), and March 2019 (180 events) from the main catalogue to compute the b-values of individual swarms using maximum curvature fit of the magnitude of completeness value (M_c). We used the Harvard CMT solutions to understand the focal mechanism of large magnitude ($>4.0 M_b$) earthquakes.

We used Zmap software (Wiemer, 2001) for analysis of earthquake data, and estimated the temporal distribution of b-value in the off Nicobar region. We estimated the b-value using the maximum likelihood method as it provides unbiased results with minimum standard deviation (Aki, 1965; Hirata, 1989; Wiemer, 2001).

4. Results

Gutenberg-Richer frequency-magnitude relationship

The Gutenberg–Richter frequency-magnitude relationship is a fundamental seismological equation that adequately describes the aftershock activity and earthquake swarms (Gutenberg and Richter, 1944). Gutenberg–Richter law defines the relationship between the number of earthquakes occurred in a time period and their magnitudes and is expressed as,

$$\log_{10} N = a - bM, \quad (1)$$

Where N is the cumulative number of earthquakes of magnitude $\geq M$, a and b are constants. The parameter a is related to earthquake productivity in a volume whereas b represents the relative distribution of large and small-magnitude earthquakes. The b-value is often computed using the Maximum Likelihood method as it provides a stable estimate (Aki, 1965; Hirata, 1989) when the number of events exceeds 50 (Utsu, 1965). In the Maximum Likelihood method, the b-value is defined as,

$$b = \frac{\log_{10} e}{\bar{M} - M_0}, \quad (2)$$

where \bar{M} is the average magnitude, M_0 represents threshold magnitude and $\log_{10} e = 0.4343$. The threshold magnitude is the minimum magnitude above which all the earthquakes are consistently detected (Rydelek and Sacks, 1989).

In the present study, 2552 events are observed in the Off Nicobar region along the volcanic arc and also in-between the sliver fault system such as ANF and the northern part of the Great Sumatra strike-slip Fault (Fig. 2). An energetic earthquake swarm occurred centred over the cratered seamount between the two major sliver fault systems ANF and GSF in January 2005 after the 2004 Sumatra event. A major earthquake occurred on 21st March 2014 (Mw 6.5), which was followed by an earthquake swarm on 21st and 22nd March 2014. After March 2014, four distinct sets of energetic swarms are observed in October 2014, November 2015, and April 2019 in the off Nicobar region (Fig. 2). The magnitude versus time graphs of individual earthquake swarms are shown in Fig. 3. Earthquake sequence are classified into three types such as I) mainshock and aftershock distribution generally show the decay in magnitude with time, II) foreshock-mainshock-aftershock distribution shows the slow build-up of seismicity before a mainshock, III) gradual increase and decrease of magnitude without any mainshock (Farrel et al., 2009). In our data, March 2014 event shows a mainshock at the beginning but systematic decay of magnitude with time is indiscernible, classifying the events as an earthquake swarm. Type I and Type II distributions are not seen for the clusters of October 2014, November 2015, and April 2019. The absence of a mainshock and increase and decrease of magnitude with time in these events suggests that these clusters are also can be classified as earthquake swarms (type III). Further, we noted that the duration of the earthquake swarm with respect to the October 2014 event is about 42 days, whereas the other swarms are of shorter duration of 1 to 2.5 days (30 to 60 hrs). We computed b-value for these earthquakes to gain insights into the volcano-tectonic activity of the region.

In the off Nicobar region, the cumulative number of shallow-focus (0-30 km) and intermediate-focus (30-100 km) earthquakes are shown in Fig. 4a during 2000-2020. Few earthquakes are observed prior to 2005; however, a significant number of earthquakes (917 events) were observed in January 2005 due to volcano-tectonic activity (Kamesh Raju et al., 2012; Kundu et al., 2012). There was a period of seismic quiescence from 2005 to 2014, which was interrupted on 21st March 2014 by an M_w 6.5 earthquake. Thereafter, several peaks in earthquake activity are observed in March 2014, October 2014, November 2015, and April 2019, indicative of the occurrence of significant swarms (Fig. 4a). The background value of threshold magnitude, M_c is 3.5 (Fig. 4b), which increases to 4 or more during earthquake swarms. A peak magnitude of M_c 4.6 is observed in 2005 swarm indicating the occurrence of a large number of events in a short duration of time window that resulted in the overlapping of small magnitude earthquakes (Kundu et al., 2012). Prior to and after 2005 swarm, the b-values are close to unity. During the 2005 swarm, the b-values are larger than 1.6 and are restored to unity in 2006 and 2007 (Fig. 4c). The b-value started decreasing from unity in 2007 to less than 0.65 in 2013. It again increases to 1.5 during March 2014 swarm and similar increase is also observed during November 2015 and March 2019 swarms but is absent for October 2014 swarm. A good correlation is observed between the b-value and M_c , periods of high b-value correspond to an increase in M_c . We also observed a systematic decrease in b-values in between the swarm events. The values are lowest just before the swarm event as in October 2013, September 2015 and January 2019 (Fig. 4c). The temporal distribution of b-value shows an overall picture of positive correlation between increase in cumulative number and increase in b-value and M_c .

We obtained the threshold magnitude ($M_c = 3.8$) and b-value (0.858) for the entire catalogue as shown in Fig. 5a. We removed the swarm events from the catalogue and re-computed the M_c and b-value resulting in 4 and 0.739 respectively (Fig. 5b). Further, we computed the b-values for individual swarms in January 2005 (Fig. 5c), March 2014, October 2014, November 2015, and April 2019 (Figs. 6a, 6b, 6c, 6d). The frequency magnitude distribution of the 2005 earthquake swarm shows bimodal characteristics having a double slope with two different b-values such as $b_1 = 1.02$ and $b_2 = 1.6$ (Fig. 5c). Previous studies suggest that these two slope values are real and not an artefact arising out of an incomplete catalogue (Kundu et al., 2012). The b value for lower magnitude range ($M_c = 4.2$ and $M_{break} = 5.2$) and higher magnitude range ($M_{break} = 5.2$ and $M_{end} = 5.8$) are 1.02 and 1.6, respectively. The b_1 (1.02) value is close to the b-value of the whole region, suggesting seismicity is of tectonic origin. The higher b_2 -value (1.6) may arise from different conditions such as i) material heterogeneity in the volcanic system (Mogi, 1962), ii) microfracture formation due to the presence of highly porous rocks (Scholz, 1968), iii) due to high thermal gradient. The presence of

fluid or increase in temperature in the region are the likely causes for the observed double slope (Kundu et al., 2012). In addition, the presence of a cratered seamount in the vicinity of this earthquake swarm suggests magmatic activity in the region (Kamesh Raju et al., 2012; Kundu et al., 2012).

The computed M_c and b-value for the March 2014 swarm are 3 and 1.39 respectively (Fig. 6a). The March 2014 events are located using OBS and ISLAND station network and nearby land station data (Aswini et al., 2020). The body wave magnitude ranges from 2 - 6.1. Here we could locate the lower magnitude events when compared to the global network data due to our OBS network. These events are classified as hybrid long-period earthquakes and suggest subsurface magma movement (Aswini et al., 2020). The high b-value supports the volcanic origin of these events. The frequency-magnitude relationship for October 2014, November 2015, and April 2019 shows bimodal characteristics similar to that observed for 2005 swarm (Figs. 6b, 6c, 6d). The lower magnitude range (between M_c and M_{break}) shows b-value less than unity, which resembles the background seismicity. Higher magnitude range (between M_{break} and M_{end}) shows b-value larger than unity similar to that observed for 2005 swarm. The b_1 and b_2 values computed for October 2014, November 2015, April 2019 swarms are (0.74, 1.36), (0.72, 1.32), (0.7, 1.5), respectively (Figs. 6b, 6c, 6d). Since the global network detects higher magnitude events more accurately, the b-value greater than one in this range can be attributed to the geological process. The bimodal magnitude distributions are typical for volcanic areas and suggest fluid-induced swarm activity (Wiemer and Wyss, 2002). This inference suggests that the presence of fluids has a significant role in the occurrence of earthquake swarms. In order to ascertain that the higher b-values are indeed resulting from the events in the near vicinity of the volcanic arc, we computed the b-value separately for the events in the near vicinity of the volcanic arc and away from it. The b-values are higher than one for the events near to the volcanic arc suggesting the dominance of volcanic component and b-value away from the arc are lesser than one indicating the dominance of tectonic component (Supplementary Figs. S1, S2).

5. Discussion

Earthquake swarms and triggered aftershocks usually occur from stress perturbation resulting from local/regional tectonic activity (Brodsky et al., 2000; Brodsky and Prejean, 2005). Swarm type of earthquake clusters are considered to be good indicators of movement of fluids or sub-surface magma movement in the earth crust (Linde and Sacks, 1998; Fischer and Horálek, 2005; Hensch et al., 2008). Several significant earthquake swarms have been reported in the Andaman-Nicobar region (Mukhopadhyay and Dasgupta, 2008; Kamesh Raju et al., 2012; Kundu et al., 2012; Diehl et al.,

2013). These swarms occurred along the ABSC (during 1983-1984, 1993-1994, 2006, 2009, and 2012), off Nicobar region (during 1982, 1986, 1998, 2005, 2014, 2015, and 2019), offshore extension of GSF (2001) and in the region proximal to Simeulue Island (2002).

The earthquake swarms observed in the off Nicobar Island region after the 2004 Sumatra event, are more abundant in number of events, and more energetic in terms of magnitude, compared to other regions of the Andaman Sea. Previous studies suggested a volcano-tectonic origin to the Jan 2005 Off Nicobar swarm that was triggered by the 2004 megathrust event (Kamesh Raju et al., 2012; Kundu et al., 2012). Several long-period hybrid events were detected by the passive OBS experiment of March 2014. The hybrid events are interpreted as events originating from subsurface tectonic and magmatic activity (Aswini et al., 2020). Later, the region has experienced three more swarms in October 2014, November 2015, and April 2019.

The temporal analysis of b-value off Nicobar region shows that b-values corresponding to 2014, 2015, and 2019 swarms are also greater than unity in the higher magnitude range (Fig. 4). Further, the b-values derived from the frequency magnitude distribution of the earthquake swarms show bi-model distribution (Fig. 6).

The variations in the b-value suggest tectonic and rheological conditions that include material heterogeneity, crack density, geothermal gradient, and applied stress (Mogi, 1962; Scholz, 1968; Wiemer and Wyss, 1997; Wyss et al., 1997; Wiemer and Katsumata, 1999; Scholz, 2015). High b-values are linked to the over pressured fluids, the presence of fractured rocks in the faulted region, material heterogeneity in the volcanic system, and high geothermal gradient system (Wiemer and Benoit, 1996; McNutt, 2004; Govoni et al., 2013). According to Mogi (1962), earthquake swarms are commonly found in the volcanic arc or other fractured faulted regions, where magma intrusions take place. The conceptual model proposed by Hill (1977) states that a complex mesh of fluid-filled fractures can yield numerous small magnitude events, but lacks a larger magnitude event. Also, especially in volcanic areas, frequency magnitude distribution shows bimodal characteristics.

High b-values related to volcanic activity have been reported from submarine eruption off coast El Hierro during 2011- 2012 (Ibáñez et al., 2012), Kirishima Shinmoe-dake, Japan (Chiba and Shimizu, 2018), Quito swarm occurred at Guagua Pichincha volcano (Legrand et al., 2004). The bimodal frequency magnitude distributions of earthquake swarms are reported at Santorini volcanic complex, Greece (Vallianatos et al, 2013), Sunset Crater volcano, Arizona (Brumbaugh et al., 2014), Mt.Redoubt volcano, Alaska (Wiemer and Wyss, 2002), Guagua Pichincha volcano, Ecuador

(Legrand et al., 2004). After the 2004 megathrust event, the magmatic activity renewed along the volcanic arc and facilitated lava eruption from the Barren Island (Sheth et al., 2009). The above inferences suggest that the bimodal distribution of b-values observed in the Off Nicobar region is indicative of a combination of tectonic and magmatic activity. The subsurface magma activity reactivated the pre-existing fault systems and cracks in the Off Nicobar region resulting in earthquake swarms.

The high-resolution bathymetry data from this region (Fig. 1) show several volcanic edifices/topographic highs. The data shows that a very large number of volcanoes between 6.2°N and 8.2°N as compared to that in the north and south in mainland Sumatra. In a recent study, Coudurier-Curveur et al (2020) suggested that the fracture zone F6a in the Wharton Basin, where one of the largest magnitude strike-slip earthquakes (M_w 8.6) occurred in 2012, might be a nascent plate boundary between India and Australia. There is a possibility of generation of excess melt when these features are subducted beneath the mantle wedge due to enhanced dehydration. Such a tectono magmatic process may also result in enhanced volcanism. However, the present day bathymetry data does not show any expression of volcanic eruptions on the seafloor. The observed cratered seamounts (Kamesh Raju et al., 2012) are indicative of magma eruption/volcanism in the recent geological past (Kamesh Raju et al., 2012; Tripathi et al., 2018, Saha, 2020). Majority of the observed seamounts in the present study are of conical shape (Fig. 7), suggesting the absence of recent volcanic eruptions. The presence of cratered seamount roughly centered on 2005 earthquake swarm is suggestive of a link between arc volcanism and the occurrence of earthquake swarm. Further, cratered submarine volcanoes also are indicative of explosive volcanism (Walter and Amelung, 2007; Kamesh Raju et al., 2012).

The sliver fault system present in the Andaman Sea also plays an important role in modulating the stress regime of the region. The 2005 swarm occurred in between the sliver faults ANF and the SF and showed both strike-slip and normal faults suggesting volcano-tectonic origin (Kamesh Raju et al., 2012; Kundu et al., 2012). After the 2004 and 2005 megathrust earthquakes, the northern portion of GSF is experiencing maximum stress change and is likely to rupture in the near future (McCloskey et al., 2005; Cattin et al., 2009). The interaction of the compressive WAF and strike-slip GSF leads to the enhancement of seismicity in the region (Singh et al., 2013). Ghosal et al. (2012) suggested that the Aceh Fault is linear for ~200 km, and may produce an earthquake of up to 7.6 magnitude in future. On the other hand, the northern strand of SF is segmented into a strike-slip, pull-apart system, and hence is likely to produce smaller earthquakes (Ghosal et al., 2012). In

general, the earthquakes associated with the GSF are right-lateral strike-slip earthquakes. The focal mechanism solution of the 21st March 2014 6.5 M_w event that occurred in the off Nicobar region shows strike-slip faulting. 2014, 2015, and 2019 swarms also show dominant strike-slip fault plane solution (Fig. 2). Strike-slip faulting near volcanic arcs is facilitated by the increase in magma eruption rate as a consequence of post-seismic relaxation of the compressional stress regime in response to megathrust earthquakes (Lupi and Miller, 2014). In the Andaman-Nicobar subduction zone, the shear component is largely accommodated by the overriding plate as a consequence of oblique subduction (Singh et al., 2013). The Strike-slip faulting provides an easy pathway for upwelling fluids and magmas, which causes an increase in volcanic activity (Lupi and Miller, 2014). In a recent study Yang et al., (2020) analysed three sets of a large magnitude of earthquake swarms that occurred in 2018, in the vicinity of Rinjani volcano and Flores thrust and attributed them to the interaction volcanic and tectonic activities. It is suggested that the reactivation of Flores thrust due to migration of magmatic fluids is one of the possible reasons for the origination of these swarms. In the off Nicobar region, reactivation of the sliver fault system could have triggered the frequent occurrence of earthquake swarms. We propose that the 2004 and 2005 megathrust events in the Sumatra region might have initiated the tectonic and volcanic activity in the off Nicobar region along the ANF and SF. We believe that the excess Coulomb stress imparted from the 2004 and 2005 megathrust earthquakes may explain the increase of seismicity in the off Nicobar region. Also, reactivation of pre-existing fault system and strain partitioning due to oblique subduction played a role in the occurrence of earthquakes in the region. The frequent occurrence of earthquake swarms in the off Nicobar region can be inferred to be the manifestation of subsurface magma movement and the associated volcano-tectonic activity along the Seulimeum strand of GSF.

6. Conclusions

The high b-values (> 1) obtained during the earthquake swarms in the off Nicobar region indicate that swarms are of volcanic origin. Further, the frequency-magnitude relation of earthquake swarms in the off Nicobar volcanic region shows bimodal distribution (double slope) indicative of combined magmatic and tectonic activity.

Bathymetry data show several seamounts of volcanic origin suggesting recent volcanic activity. We propose that the 2004 and 2005 megathrust earthquakes and the 2014 event of 6.5 M_w occurred in the Off Nicobar region are some of the causative factors that imparted magmatic pulsation in the volcanic arc, leading to earthquake swarms in the off Nicobar region.

The reactivation of the sliver fault system induced by sub-surface magma movement in the Andaman Sea volcanic arc region provides favourable tectonic and stress regime for the occurrence of frequent earthquake swarms. In the off Nicobar region, this tectono-magmatic engineering occurred preferentially along the Seulimeum strand of GSF.

Acknowledgements

We thank Prof. Sunil Kumar Singh, Director of CSIR-NIO, Goa and Dr. M Ravichandran, Director of NCPOR, Goa for support and encouragement. We thank Dr. Graindorge and Prof. Satish Singh, IGP, Paris, for providing published bathymetry grid data in the NW Sumatra region. We thank the reviewers for the constructive comments and for the insights; they enabled us to improve the manuscript. Figures were prepared using the GMT software package (Wessel & Smith, 1998). KKA thanks Department of Science and Technology (DST), India for providing the Inspire Fellowship. The work was performed under the GENIAS (CSIR-NGRI and CSIR-NIO) and MLP1703 project of CSIR-NIO. This is a CSIR-NIO contribution xxxx.

References

- Aki, K., 1965. Maximum likelihood estimate of b in the formula $\log N = a - bM$ and its confidence limits. *Bull. Seismol. Soc. Am.* 43, 237-239.
- Ammon, C.J., Ji, C., Thio, H.-k., Robinson, D., Ni, S., Hjorleifsdottir, V., Kanamori, H., Lay, T., Das, S., Helmberger, D., Ichinose, G., Polet, J., Wald, D., 2005. Rupture Process of the 2004 Sumatra-Andaman Earthquake. *Science* 1133, 1133-1140.
- Aswini, K.K., Dewangan, P., Kamesh Raju, K.A., Yatheesh, V., Singha, P., Reddy, R., Arya, L., 2020. Hybrid long-period volcanic events observed in off Nicobar region, the Andaman Sea from a passive OBS experiment, EGU General Assembly Conference Abstracts, p. 654.
- Banerjee, P., Pollitz, F., Nagarajan, B., Burgmann, R., 2007. Coseismic Slip Distributions of the 26 December 2004 Sumatra-Andaman and 28 March 2005 Nias Earthquakes from GPS Static Offsets. *Bull. Seismol. Soc. Am.* 97, S86-S102.
- Bellier, O., Sébrier, M., Pramumijoyo, S., Beaudouin, T., Harjono, H., Bahar, I., Forni, O., 1997. Paleoseismicity and seismic hazard along the Great Sumatran Fault (Indonesia). *J. Geodyn.* 24, 169-183.
- Brodsky, E.E., Karakostas, V., Kanamori, H., 2000. A new observation of dynamically triggered regional seismicity: Earthquakes in Greece following the August 1999 Izmit, Turkey earthquake. *Geophys. Res. Lett.* 27, 2741-2744.
- Brodsky, E.E., Prejean, S.G., 2005. New constraints on mechanisms of remotely triggered seismicity at Long Valley Caldera. *J. Geophys. Res.: Solid Earth* 110, B04302.
- Brumbaugh, D.S., Hodge, B.E., Linville, L., Cohen, A., 2014. Analysis of the 2009 earthquake swarm near Sunset Crater volcano, Arizona. *J. Volcanol. Geotherm. Res.* 285, 18-28.
- Cattin, R., Chamot-Rooke, N., Pubellier, M., Rabaute, A., Delescluse, M., Vigny, C., Fleitout, L., Dubernet, P., 2009. Stress change and effective friction coefficient along the Sumatra-Andaman-Sagaing fault system after the 26 December 2004 ($M_w = 9.2$) and the 28 March 2005 ($M_w = 8.7$) earthquakes. *Geochem. Geophys. Geosyst.* 10, Q03011.
- Chiba, K., Shimizu, H., 2018. Spatial and temporal distributions of b -value in and around Shinmoe-dake, Kirishima volcano, Japan. *Earth Planets Space* 70, 122.
- Cochran, J.R., 2010. Morphology and tectonics of the Andaman Forearc, northeastern Indian Ocean. *Geophys. J. Int.* 182, 631-651.
- Coudurier-Curveur, A., Karakaş, Ç., Singh, S. C., Tapponnier, P., Carton, H., Hananto, N., 2020. Is There a Nascent Plate Boundary in the Northern Indian Ocean?. *Geophys. Res. Lett.* 47, 7.
- Curry, J.R., 2005. Tectonics and history of the Andaman Sea region. *J. Asian Earth Sci.* 25, 187-232.
- Dewangan, P., Reddy, R., Kamesh Raju, K.A., Singha, P., Aswini, K.K., Yatheesh, V., Samudrala, K., Shuhail, M., 2018. Nature of the ambient noise, site response, and orientation of ocean-bottom seismometers (OBSs): Scientific results of a passive seismic experiment in the Andaman Sea. *Bull. Seismol. Soc. Am.* 108, 248-259.

- Diehl, T., Waldhauser, F., Cochran, J.R., Kamesh Raju, K.A., Seeber, L., Schaff, D., Engdahl, E.R., 2013. Back-arc extension in the Andaman Sea: Tectonic and magmatic processes imaged by high-precision teleseismic double-difference earthquake relocation. *J. Geophys. Res.: Solid Earth* 118, 2206-2224.
- Engdahl, E.R., van der Hilst, R., Buland, R., 1998. Global teleseismic earthquake relocation with improved travel times and procedures for depth determination. *Bull. Seismol. Soc. Am.* 88, 722-743.
- Farrell, J., Husen, S., Smith, R.B., 2009. Earthquake swarm and b-value characterization of the Yellowstone volcano-tectonic system. *J. Volcanol. Geotherm. Res.* 188, 260-276.
- Farrell, J., Smith, R.B., Taira, T.a., Chang, W.L., Puskas, C.M., 2010. Dynamics and rapid migration of the energetic 2008–2009 Yellowstone Lake earthquake swarm. *Geophys. Res. Lett.* 37, L19305.
- Fischer, T., Horálek, J., 2005. Slip-generated patterns of swarm microearthquakes from West Bohemia/Vogtland (central Europe): Evidence of their triggering mechanism? *J. Geophys. Res.: Solid Earth* 110, B5.
- Frohlich, C., Davis, S.D., 1993. Teleseismic b values; Or, much ado about 1.0. *J. Geophys. Res.: Solid Earth* 98, 631-644.
- Fujii, Y., Satake, K., 2007. Tsunami Source of the 2004 Sumatra–Andaman Earthquake Inferred from Tide Gauge and Satellite Data. *Bull. Seismol. Soc. Am.* 97, S192-S207.
- Gahalaut, V., Nagarajan, B., Catherine, J., Kumar, S., 2006. Constraints on 2004 Sumatra–Andaman earthquake rupture from GPS measurements in Andaman–Nicobar Islands. *Earth Planet. Sci. Lett.* 242, 365-374.
- Gahalaut, V.K., Jade, S., Catherine, J.K., Gireesh, R., Ananda, M.B., Kumar, P., Narsaiah, M., Jafri, S.S.H., Ambikapathy, A., Bansal, A., Chadha, R.K., Gupta, D.C., Nagarajan, B., Kumar, S., 2008. GPS measurements of postseismic deformation in the Andaman-Nicobar region following the giant 2004 Sumatra-Andaman earthquake. *J. Geophys. Res.* 113, B08401.
- Ghosal, D., Singh, S.C., Chauhan, A.P.S., Hananto, N.D., 2012. New insights on the offshore extension of the Great Sumatran fault, NW Sumatra, from marine geophysical studies. *Geochem. Geophys. Geosyst.* 13, Q0AF06.
- Govoni, A., Passarelli, L., Braun, T., Maccaferri, F., Moretti, M., Lucente, F.P., Rivalta, E., Cesca, S., Hainzl, S., Woith, H., De Gori, P., Dahm, T., Chiarabba, C., Margheriti, L., 2013. Investigating the Origin of Seismic Swarms. *Eos, Transactions* 94, 361-362.
- Gutenberg, B., Richter, C.F., 1944. Frequency of earthquakes in California *Bull. Seismol. Soc. Am.* 34, 185-188.
- Hensch, M., Riedel, C., Reinhardt, J., Dahm, T., 2008. Hypocenter migration of fluid-induced earthquake swarms in the Tjörnes Fracture Zone (North Iceland). *Tectonophysics* 447, 80-94.
- Hill, D.P., 1977. A model for earthquake swarms. *J. Geophys. Res. (1896-1977)* 82, 1347-1352.

- Hirata, T., 1989. A correlation between the b value and the fractal dimension of earthquakes. *J. Geophys. Res.: Solid Earth* 94, 7507-7514.
- Ibáñez, J.M., De Angelis, S., Díaz-Moreno, A., Hernández, P., Alguacil, G., Posadas, A., Pérez, N., 2012. Insights into the 2011–2012 submarine eruption off the coast of El Hierro (Canary Islands, Spain) from statistical analyses of earthquake activity. *Geophys. J. Int.* 191, 659-670.
- Kamesh Raju, K.A., Murty, G.P.S., Amarnath, D., Kumar, M.L.M., 2007. The west Andaman fault and its influence on the aftershock pattern of the recent megathrust earthquakes in the Andaman-Sumatra region. *Geophys. Res. Lett.* 34, 1-5.
- Kamesh Raju, K.A., Ramprasad, T., Rao, P.S., Ramalingeswara Rao, B., Varghese, J., 2004. New insights into the tectonic evolution of the Andaman basin, northeast Indian Ocean. *Earth Planet. Sci. Lett.* 221, 145-162.
- Kamesh Raju, K.A., Ray, D., Mudholkar, A., Murty, G.P.S., Gahalaut, V.K., Samudrala, K., Paropkari, A.L., Ramachandran, R., Surya Prakash, L., 2012. Tectonic and volcanic implications of a cratered seamount off Nicobar Island, Andaman Sea. *J. Asian Earth Sci.* 56, 42-53.
- Kundu, B., Legrand, D., Gahalaut, K., Gahalaut, V.K., Mahesh, P., Kamesh Raju, K.A., Catherine, J.K., Ambikapathy, A., Chadha, R.K., 2012. The 2005 volcano-tectonic earthquake swarm in the Andaman Sea: Triggered by the 2004 great Sumatra-Andaman earthquake. *Tectonics* 31, 1-11.
- Lay, T., Ward, S.N., Kanamori, H., Ammon, C.J., Nettles, M., Ekström, G., Aster, R.C., Bilek, S.L., Beck, S.L., Brudzinski, M.R., Deshon, H.R., Butler, R., Satake, K., Sipkin, S., 2005. The great Sumatra-Andaman earthquake of 26 December 2004. *Science* 308, 1127-1132.
- Legrand, D., Villagómez, D., Yepes, H., Calahorrano, A., 2004. Multifractal dimension and b value analysis of the 1998–1999 Quito swarm related to Guagua Pichincha volcano activity, Ecuador. *J. Geophys. Res.: Solid Earth* 109, B1.
- Linde, A.T., Sacks, I.S., 1998. Triggering of volcanic eruptions. *Nature* 395, 888-890.
- Lupi, M., Miller, S.A., 2014. Short-lived tectonic switch mechanism for long-term pulses of volcanic activity after mega-thrust earthquakes. *Solid Earth* 5, 13-24.
- McCloskey, J., Nalbant, S.S., Steacy, S., 2005. Earthquake risk from co-seismic stress. *Nature* 434, 291-291.
- McNutt, S.R., 2004. Volcanic Seismology. *Annu. Rev. Earth. Planet. Sci.* 33, 461-491.
- Mogi, K., 1962. Magnitude-frequency relation for elastic shocks accompanying fractures of various materials and some related problems in earthquakes. *Bull. Earthq. Res. Inst., Univ. Tokyo* 40.
- Mukhopadhyay, B., Dasgupta, S., 2008. Swarms in Andaman Sea, India - A seismotectonic analysis. *Acta Geophys.* 56, 1000-1014.
- Rhie, J., Dreger, D., Bürgmann, R., Romanowicz, B., 2007. Slip of the 2004 Sumatra–Andaman Earthquake from Joint Inversion of Long-Period Global Seismic Waveforms and gps Static Offsets. *Bull. Seismol. Soc. Am.* 97, S115-S127.

- Rydelek, P.A., Sacks, I.S., 1989. Testing the completeness of earthquake catalogues and the hypothesis of self-similarity. *Nature* 337, 251-253.
- Saha, A., Mudholkar, A. V., Kamesh Raju, K. A., 2020. Magma genesis at Andaman volcanic arc regime, Northeastern Indian Ocean: Role of slab-mantle interaction. *IUGS*. 43, 323-334.
- Scholz, C.H., 1968. The frequency-magnitude relation of microfracturing in rock and its relation to earthquakes. *Bull. Seismol. Soc. Am.* 58, 399-415.
- Scholz, C.H., 2015. On the stress dependence of the earthquake b value. *Geophys. Res. Lett.* 42, 1399-1402.
- Sheth, H.C., Ray, J.S., Bhutani, R., Kumar, A., Smitha, R.S., 2009. Volcanology and eruptive styles of Barren Island: an active mafic stratovolcano in the Andaman Sea, NE Indian Ocean. *Bull. Volcanol.* 71, 1021.
- Sieh, K., Natawidjaja, D., 2000. Neotectonics of the Sumatran fault, Indonesia. *J. Geophys. Res.: Solid Earth* 105, 28295-28326.
- Sieh, K., Natawidjaja, D.H., Meltzner, A.J., Shen, C.-C., Cheng, H., Li, K.-S., Suwargadi, B.W., Galetzka, J., Philibosian, B., Edwards, R.L., 2008. Earthquake Supercycles Inferred from Sea-Level Changes Recorded in the Corals of West Sumatra. *Science* 322, 1674-1678.
- Silva, R., Ferreira, T., Medeiros, A., Carmo, R., Luis, R., Wallenstein, N., Bean, C., Sousa, R., 2015. Chapter 17 Seismic activity on São Miguel Island volcano-tectonic structures (Azores archipelago). *Geol. Soc. Lon. Mem.* 44, 227.
- Singh, S.C., 2005. Sumatra earthquake research indicates why rupture propagated northward. *Eos* 86, 497-502.
- Singh, S.C., Carton, H., Tapponnier, P., Hananto, N.D., Chauhan, A.P.S., Hartoyo, D., Bayly, M., Moeljopranoto, S., Bunting, T., Christie, P., Lubis, H., Martin, J., 2008. Seismic evidence for broken oceanic crust in the 2004 Sumatra earthquake epicentral region. *Nat. Geosci.* 1, 777-781.
- Singh, S.C., Chauhan, A.P.S., Calvert, A.J., Hananto, N.D., Ghosal, D., Rai, A., Carton, H., 2012. Seismic evidence of bending and unbending of subducting oceanic crust and the presence of mantle megathrust in the 2004 Great Sumatra earthquake rupture zone. *Earth Planet. Sci. Lett.* 321-322, 166-176.
- Singh, S.C., Moeremans, R., McArdle, J., Johansen, K., 2013. Seismic images of the sliver strike-slip fault and back thrust in the Andaman-Nicobar region. *J. Geophys. Res.: Solid Earth* 118, 5208-5224.
- Singha, P., Dewangan, P., Kamesh Raju, K.A., Aswini, K.K., Ramakrushana Reddy, T., 2019. Geometry of the Subducting Indian Plate and Local Seismicity in the Andaman Region from the Passive OBS Experiment. *Geometry of the Subducting Indian Plate and Local Seismicity in the Andaman Region. Bull. Seismol. Soc. Am.* 109, 797-811.
- Srijayanthi, G., Kumar, M. R., Sirisha, T., Sushini, K., Prasad, G. S., Raju, P. S., Singh, A., Rao, N. P., 2012. The ISLANDS Network in the Andaman-Nicobar Subduction Zone. *Seismol. Res. Lett.* 83, 686-696.

- Subarya, C., Chlieh, M., Prawirodirdjo, L., Avouac, J.P., Bock, Y., Sieh, K., Meltzner, A.J., Natawidjaja, D.H., McCaffrey, R., 2006. Plate-boundary deformation associated with the great Sumatra-Andaman earthquake. *Nature* 440, 46-51.
- Toda, S., Stein, R.S., Sagiya, T., 2002. Evidence from the ad 2000 Izu islands earthquake swarm that stressing rate governs seismicity. *Nature* 419, 58-61.
- Tripathi, S., Nagendran, G., Karthikeyan, M., K. Tripathy, S., Varghese, S., Raghav, S., S, R., 2018. Morphology of submarine volcanic seamounts from inner volcanic arc of Andaman Sea. *Indian J. Geosci.* 71(3), 451–470.
- Utsu, T., 1965. A method for determining the value of b in formula $\log N=a-bM$ showing the magnitude-frequency relation for earthquakes. *Geophys. Bull. Hokkaido Univ.* 13, 99-103.
- Vallianatos, F., Michas, G., Papadakis, G., Tzani, A., 2013. Evidence of non-extensivity in the seismicity observed during the 2011–2012 unrest at the Santorini volcanic complex, Greece. *Nat. Hazards Earth Syst. Sci.* 13, 177-185.
- Walter, T.R., Amelung, F., 2007. Volcanic eruptions following $M \geq 9$ megathrust earthquakes: Implications for the Sumatra-Andaman volcanoes. *Geology* 35, 539-542.
- Wessel, P., Smith, W.H.F., 1998. New, improved version of generic mapping tools released. *Eos*, 79, 579-579.
- Wiemer, S., 2001. A software package to analyze seismicity: ZMAP. *Seismol. Res. Lett.* 72, 373-382.
- Wiemer, S., Benoit, J., 1996. Mapping the b value anomaly at 100 km depth in the Alaska and New Zealand subduction zones. *Geophys. Res. Lett.* 23, 13.
- Wiemer, S., Katsumata, K., 1999. Spatial variability of seismicity parameters in aftershock zones. *J. Geophys. Res.* 104, 13135-13152.
- Wiemer, S., Wyss, M., 1997. Mapping the frequency-magnitude distribution in asperities: An improved technique to calculate recurrence times. *J. Geophys. Res.* 102, 15115–15128.
- Wiemer, S., Wyss, M., 2002. Mapping spatial variability of the frequency-magnitude distribution of earthquakes, in: Dmowska, R., Saltzman, B. (Eds.), *Adv. Geophys.* 45, 259-V.
- Wyss, M., Hasegawa, A., Nakajima, J., 2001. Source and path of magma for volcanoes in the subduction zone of northeastern Japan. *Geophys. Res. Lett.* 28, 1819-1822.
- Wyss, M., Shimazaki, K., Wiemer, S., 1997. Mapping active magma chambers by b values beneath the off-Ito volcano, Japan. *J. Geophys. Res.* 102, 413-420.
- Yang, X., Singh, S. C., Tripathi, A., 2020. Did the Flores backarc thrust rupture offshore during the 2018 Lombok earthquake sequence in Indonesia?. *Geophys. J. Int.* 221, 758-768.
- Zobin, V.M., Nishimura, Y., Miyamura, J.i., 2005. The nature of volcanic earthquake swarm preceding the 2000 flank eruption at Usu volcano, Hokkaido, Japan. *Geophys. J. Int.* 163, 265-275.

Figure Captions

Figure 1: Tectonic map of Andaman-Sumatra subduction with high resolution multibeam bathymetry data. Major tectonic elements such as Great Sumatra Fault (GSF), West Andaman Fault (WAF), Andaman-Nicobar Fault (ANF), Andaman Backarc Spreading Centre (ABSC), Andaman Transform Fault (ATF), Sagaing Fault (SGF), Sewell Seamount (SS) and Alcock Seamount (AS) are marked. Red triangles represent volcanoes. Study area is marked with black boarder lines.

Figure 2: Compiled seismicity map of off Nicobar region with earthquake swarm location. Yellow circles indicate 2005 swarm, blue circles indicate 2014 swarm, green circles indicate October 2014 swarm, brown circle indicates November 2015 swarm, pink circle indicates 2019 swarm.

Figure 3: Magnitude versus time plot of March 2014, October 2014, November 2015, April 2019 swarms.

Figure 4: (a) Cumulative number of earthquakes with time (during 2000 -2020). (b) Temporal distribution of Magnitude of completeness value off Nicobar region. (c) Temporal distribution b-value off Nicobar region.

Figure 5: (a) Cumulative magnitude-frequency of entire earthquake catalogue off Nicobar region. (b) Cumulative magnitude-frequency of earthquake location without earthquake swarms off Nicobar region. (c) Cumulative magnitude-frequency of January 2005 swarm. Squares and triangles represent cumulative number of earthquakes and first derivatives of the data to determine magnitude of completeness, respectively.

Figure 6: (a) Cumulative magnitude-frequency of March 2014 swarm (b) Cumulative magnitude-frequency of October 2014 swarm (c) Cumulative magnitude-frequency of November 2015 swarm. (d) Cumulative magnitude-frequency of April 2019 swarm. Squares and triangles represent cumulative number of earthquakes and first derivatives of the data to determine magnitude of completeness, respectively.

Figure 7: Color-coded multibeam bathymetry image of volcanic craters presents off Nicobar region. Profiles across the crater seamounts are also shown.

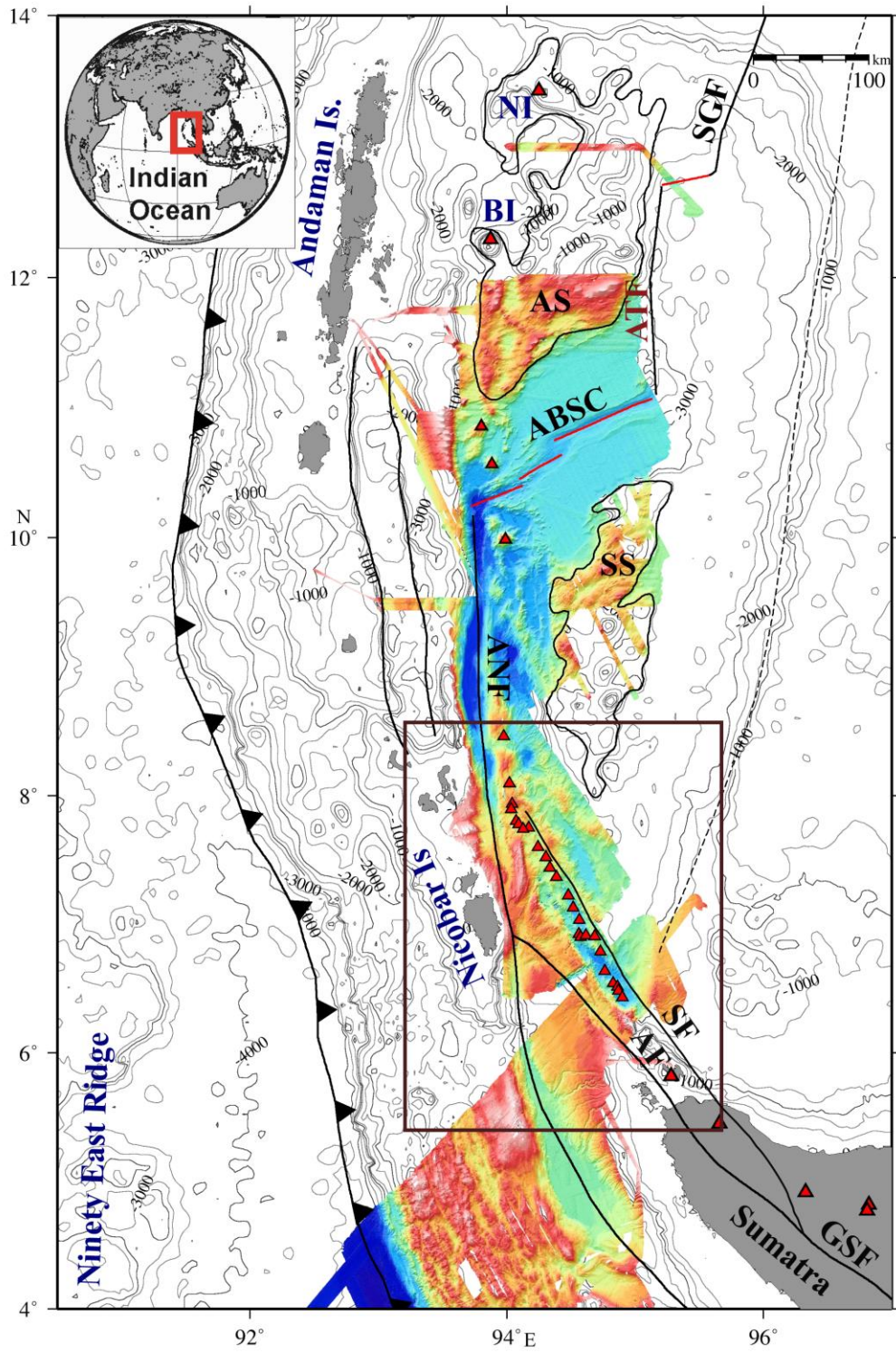


Figure 1

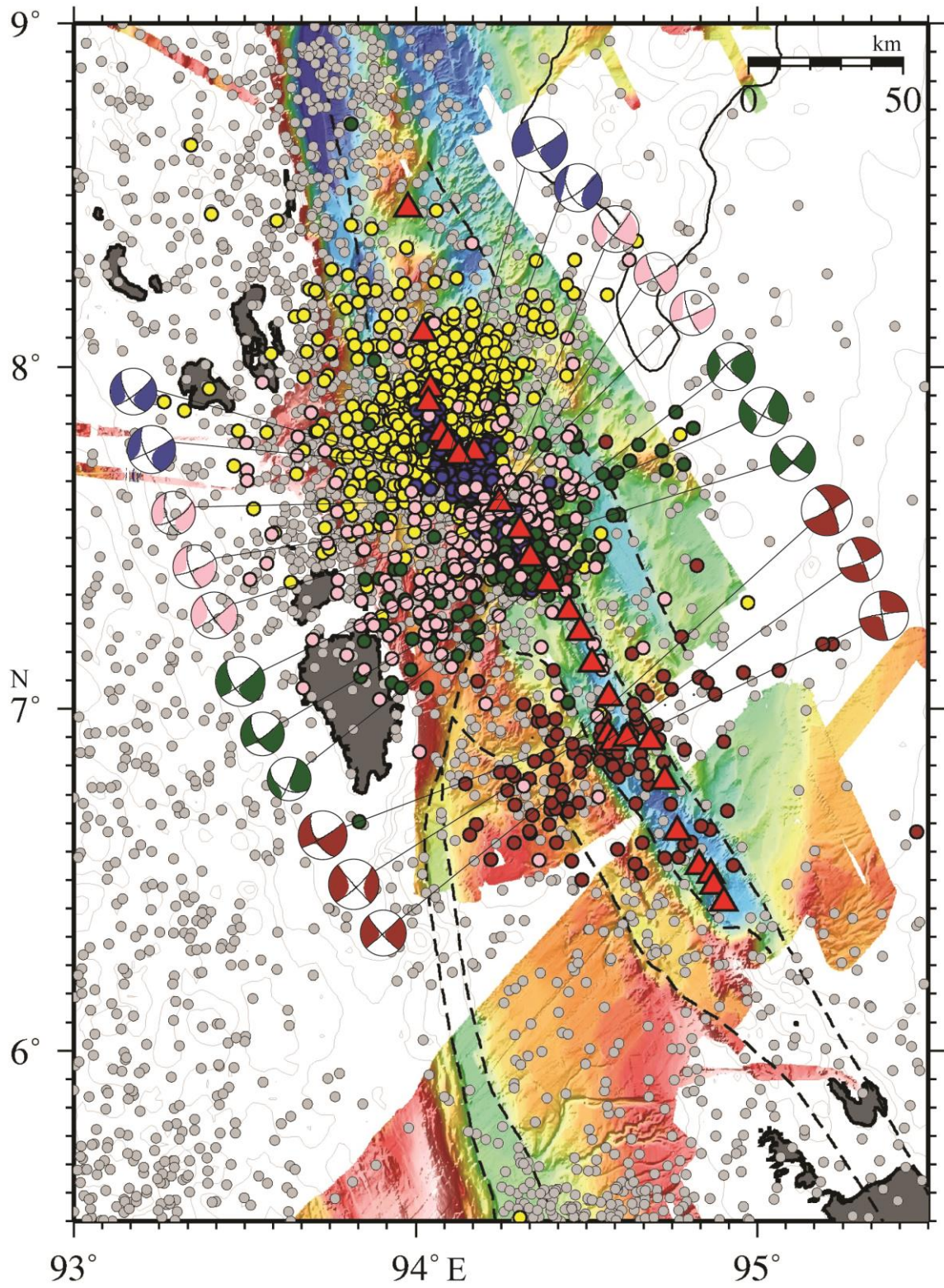


Figure 2

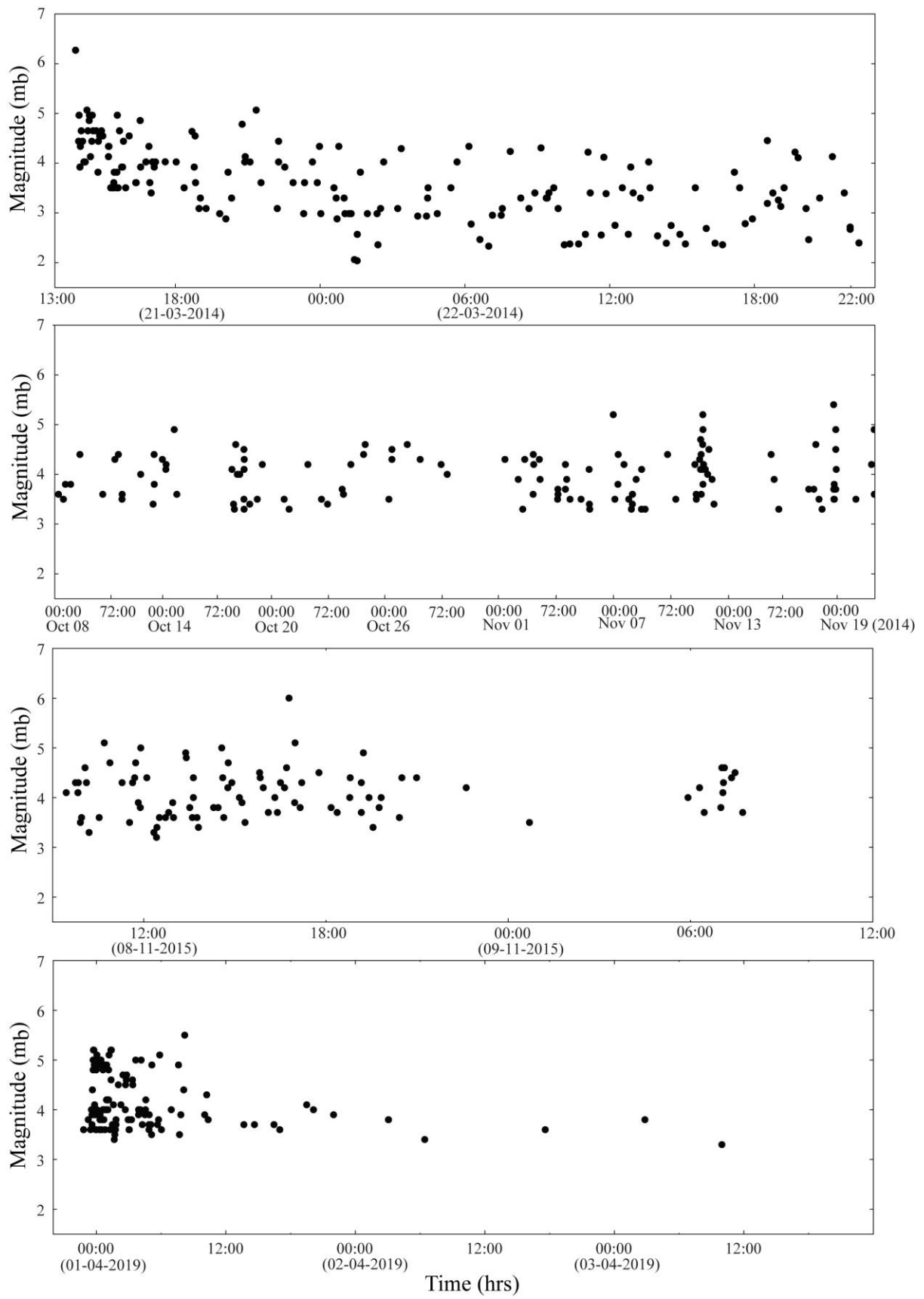


Figure 3

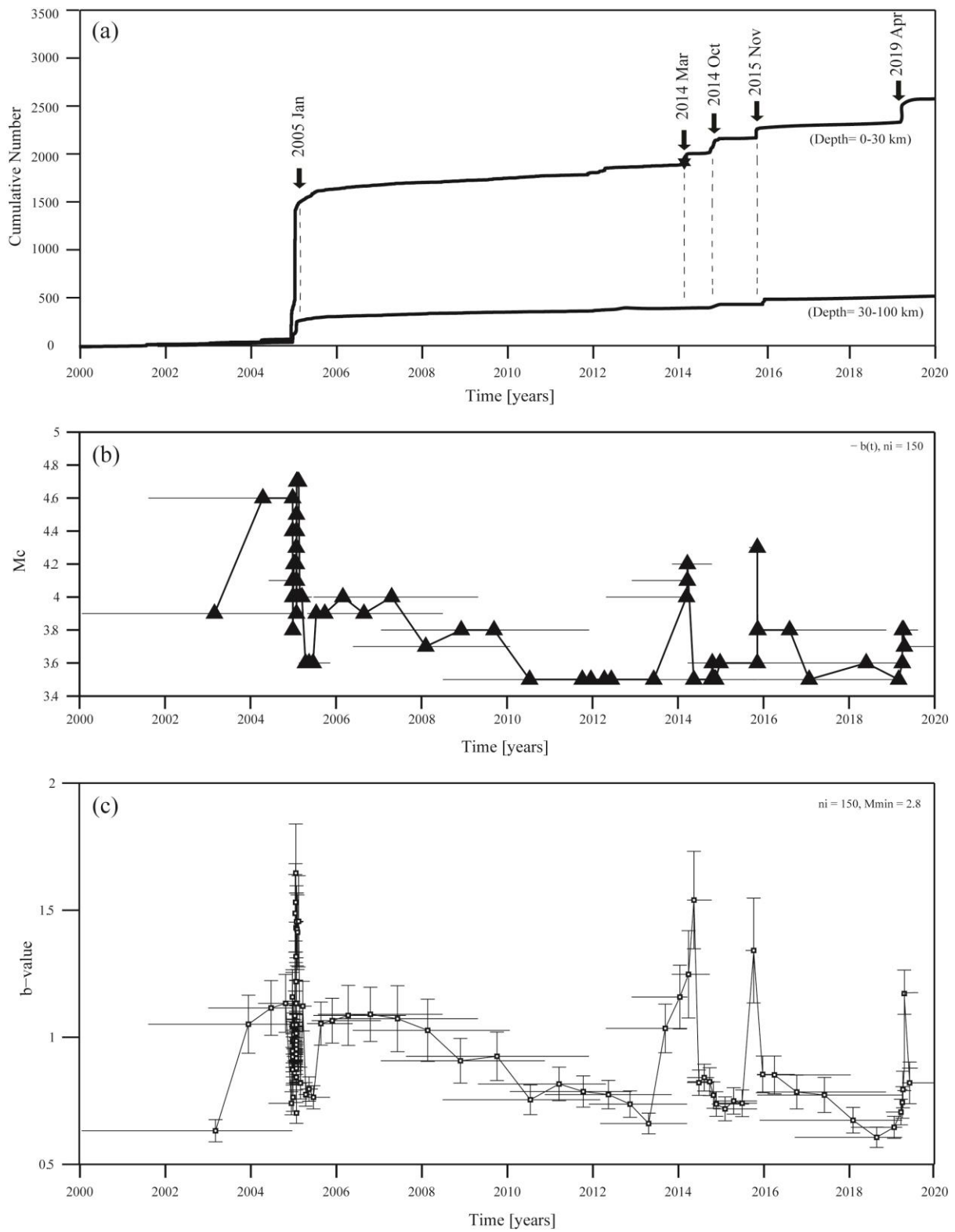


Figure 4

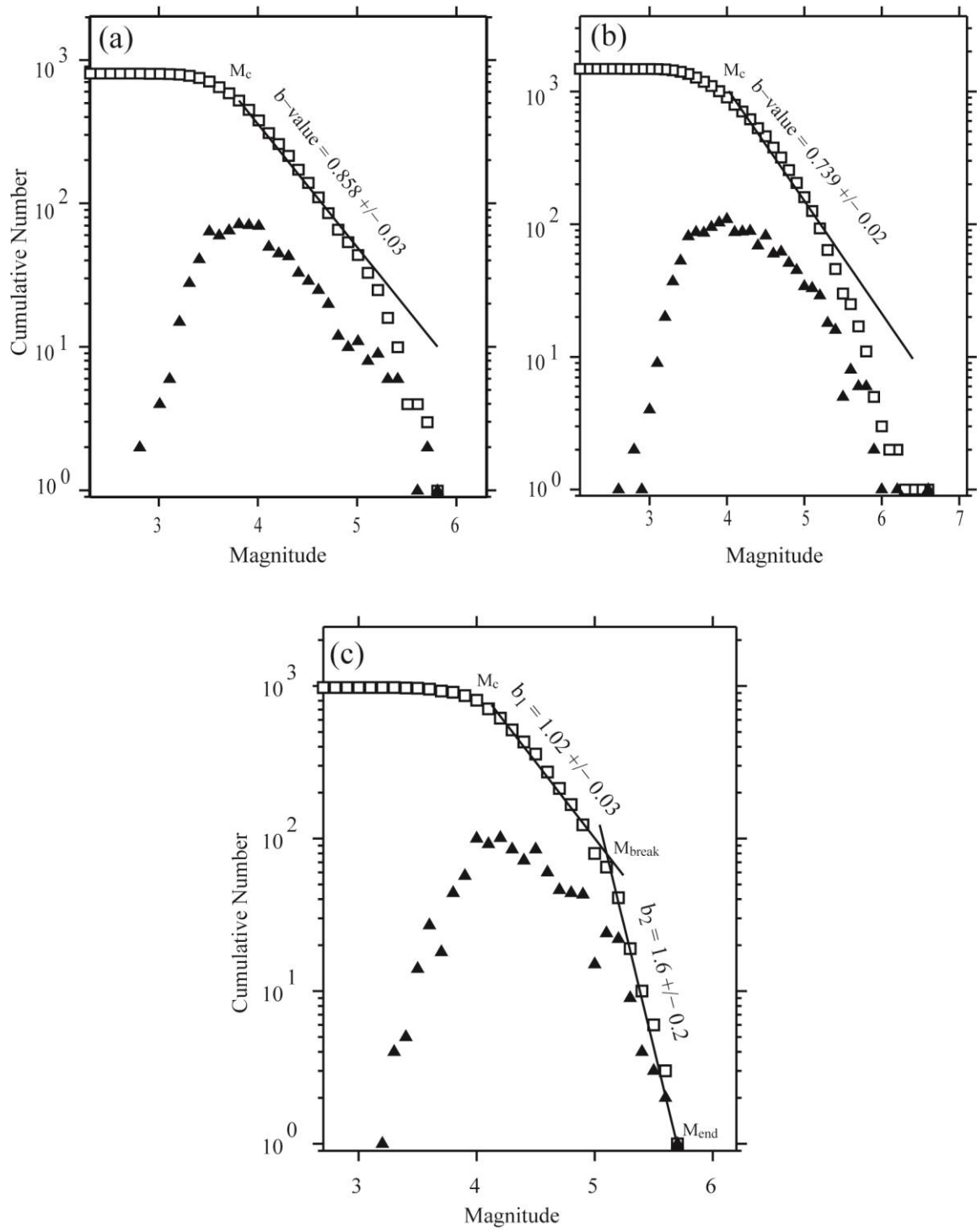


Figure 5

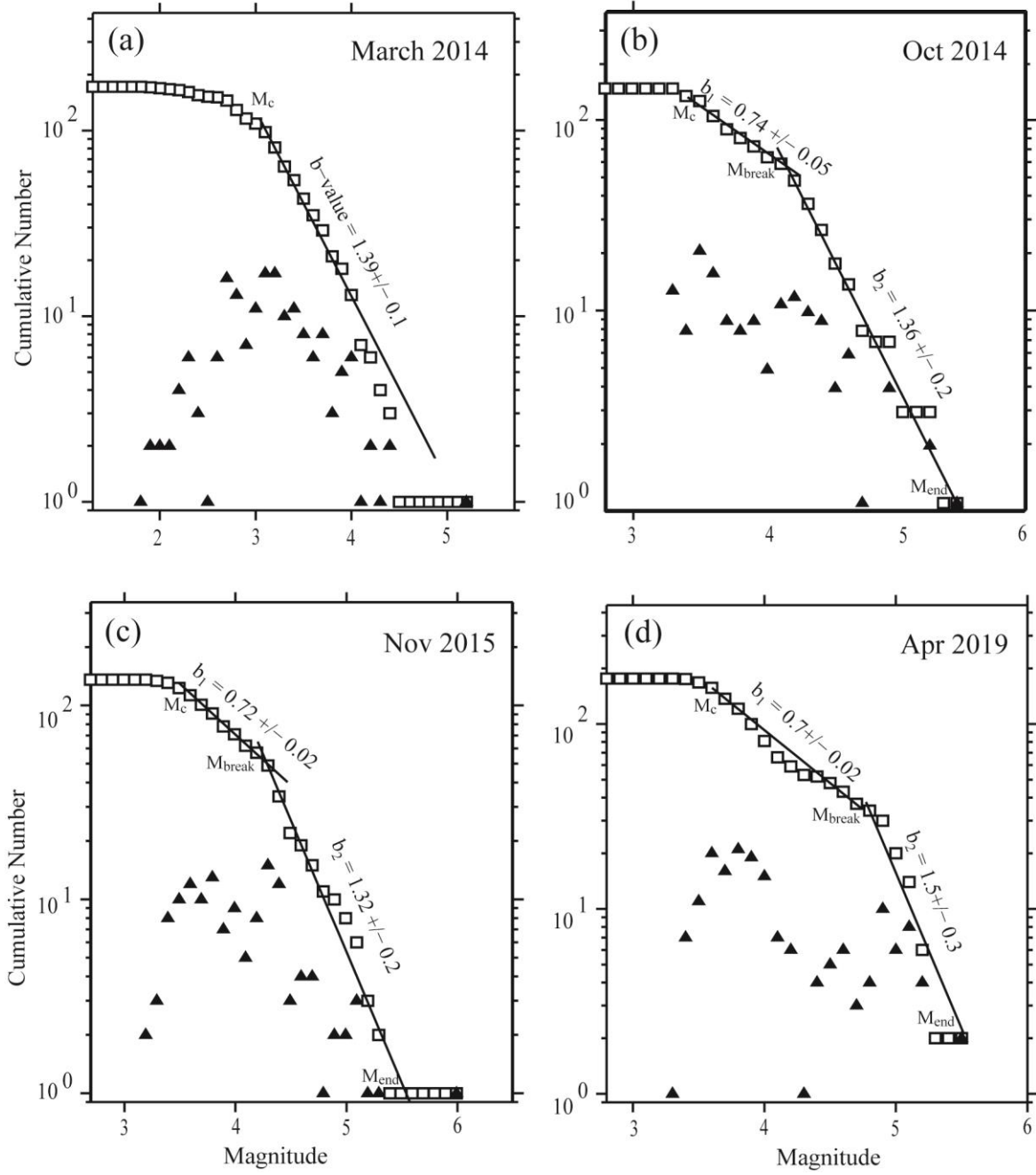


Figure 6

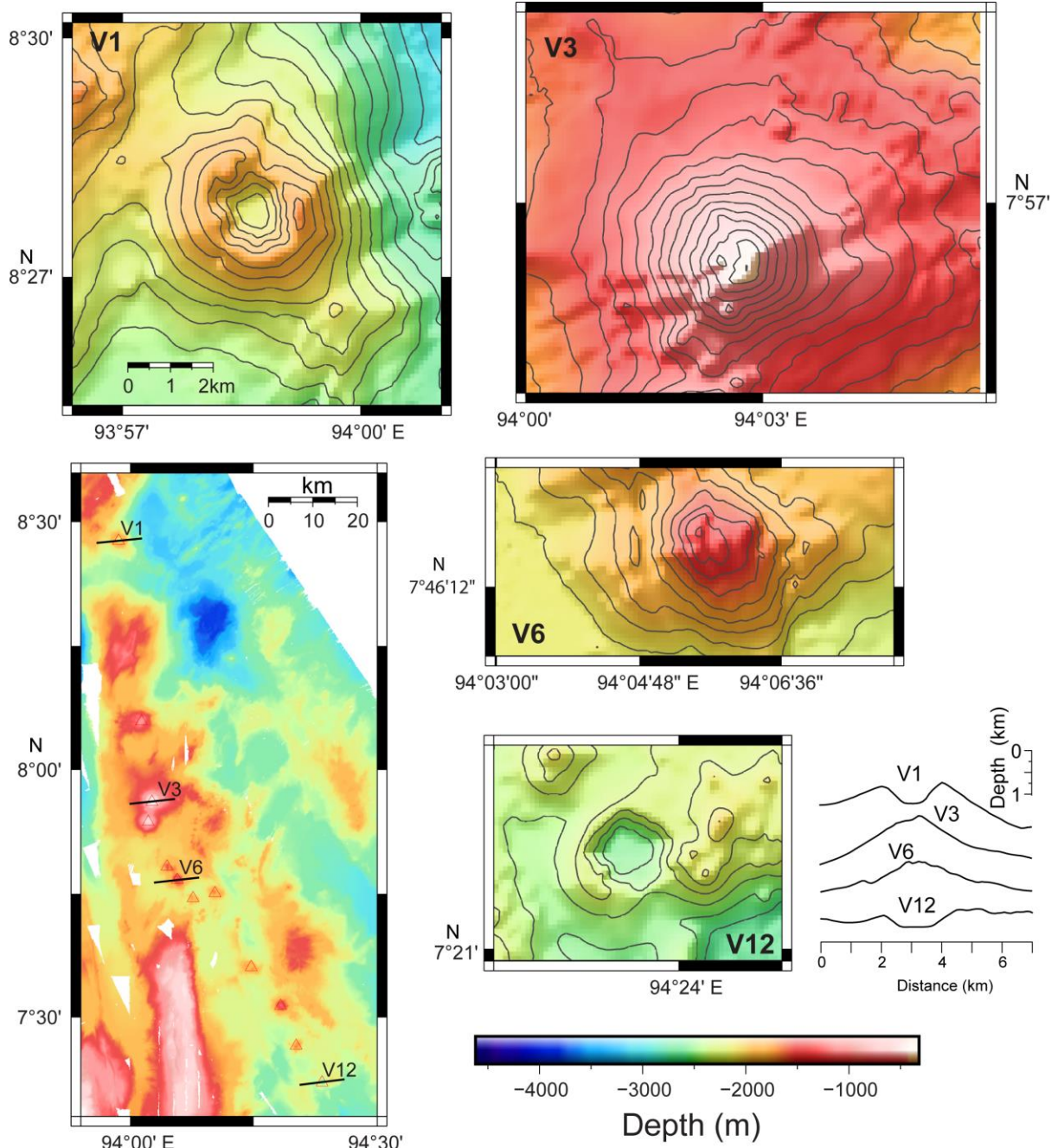


Figure 7

Journal of Asian Earth Sciences

Supplementary Information for

Seismotectonic evaluation of off Nicobar earthquake swarms, Andaman Sea

Karanam Kattil Aswini^{1,2}, Kattoju Atchuta Kamesh Raju^{1,3*}, Pawan Dewangan¹, Vadakkeyakath Yatheesh¹,
Pabitra Singha¹, Telluri Ramakrushana Reddy¹

¹*CSIR-National Institute of Oceanography, Dona Paula, Goa 403004, India*

²*School of Earth, Ocean and Atmospheric Sciences, Goa University, Taleigao Plateau, Goa 403206, India*

³*National Centre for Polar and Ocean Research, Ministry of Earth Sciences, Vasco-da-Gama, Goa 403804, India*

*Corresponding author. E-mail: kameshraju@gmail.com, kamesh@ncpor.res.in

Contents of this file

Figures S1 to S2

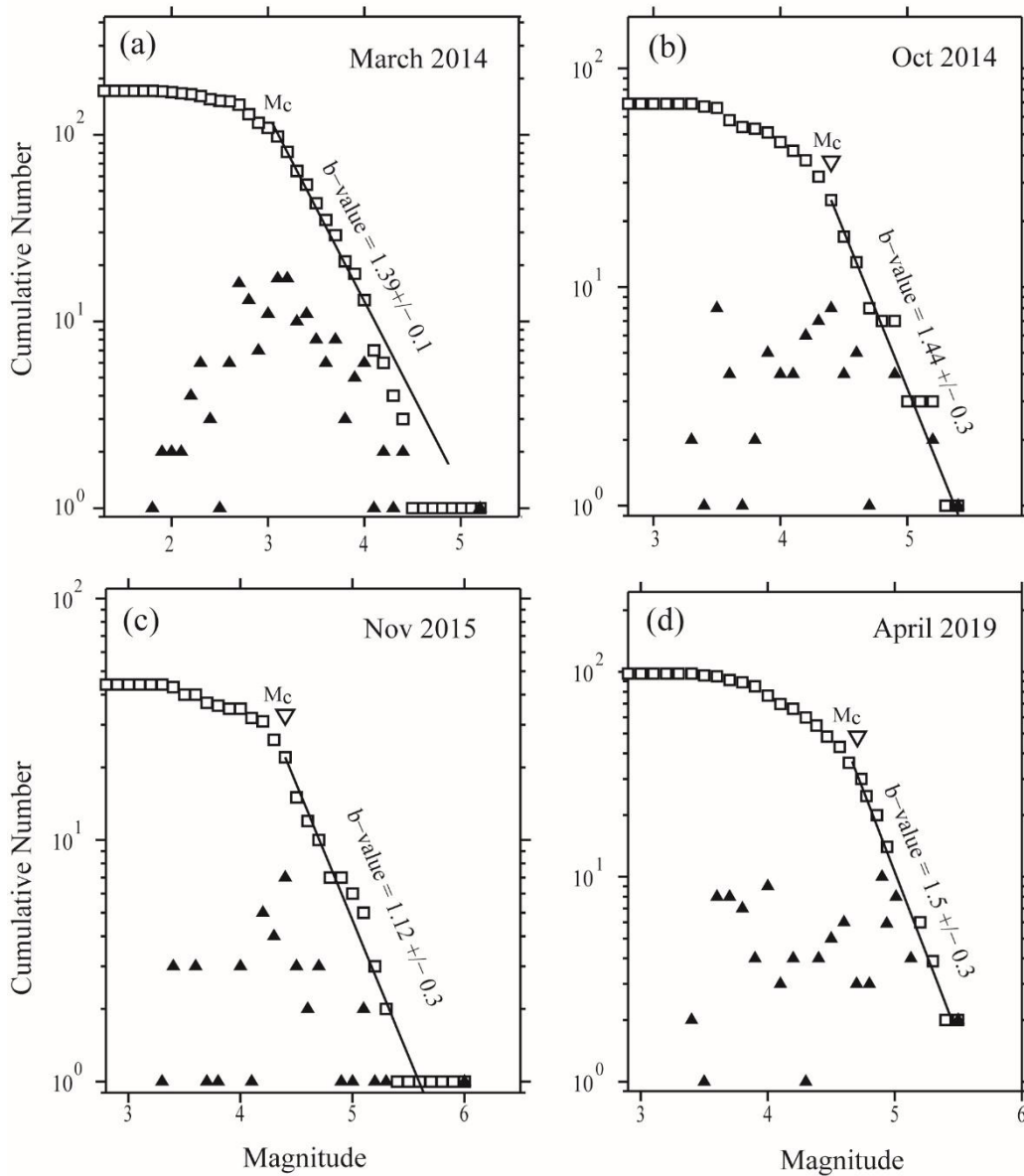


Figure S1. Cumulative magnitude-frequency and b-value of (a) March 2014, (b) October 2014, (c) November 2015, (d) April 2019 swarm in the vicinity of volcanic arc. We estimated the b-value using maximum likelihood method using Zmap software. For calculating b-value distribution for the earthquake swarm we have chosen the maximum curvature fit of magnitude of completeness value (M_c). Squares and triangles represent cumulative number of earthquakes and first derivatives of the data to determine magnitude of completeness, respectively.

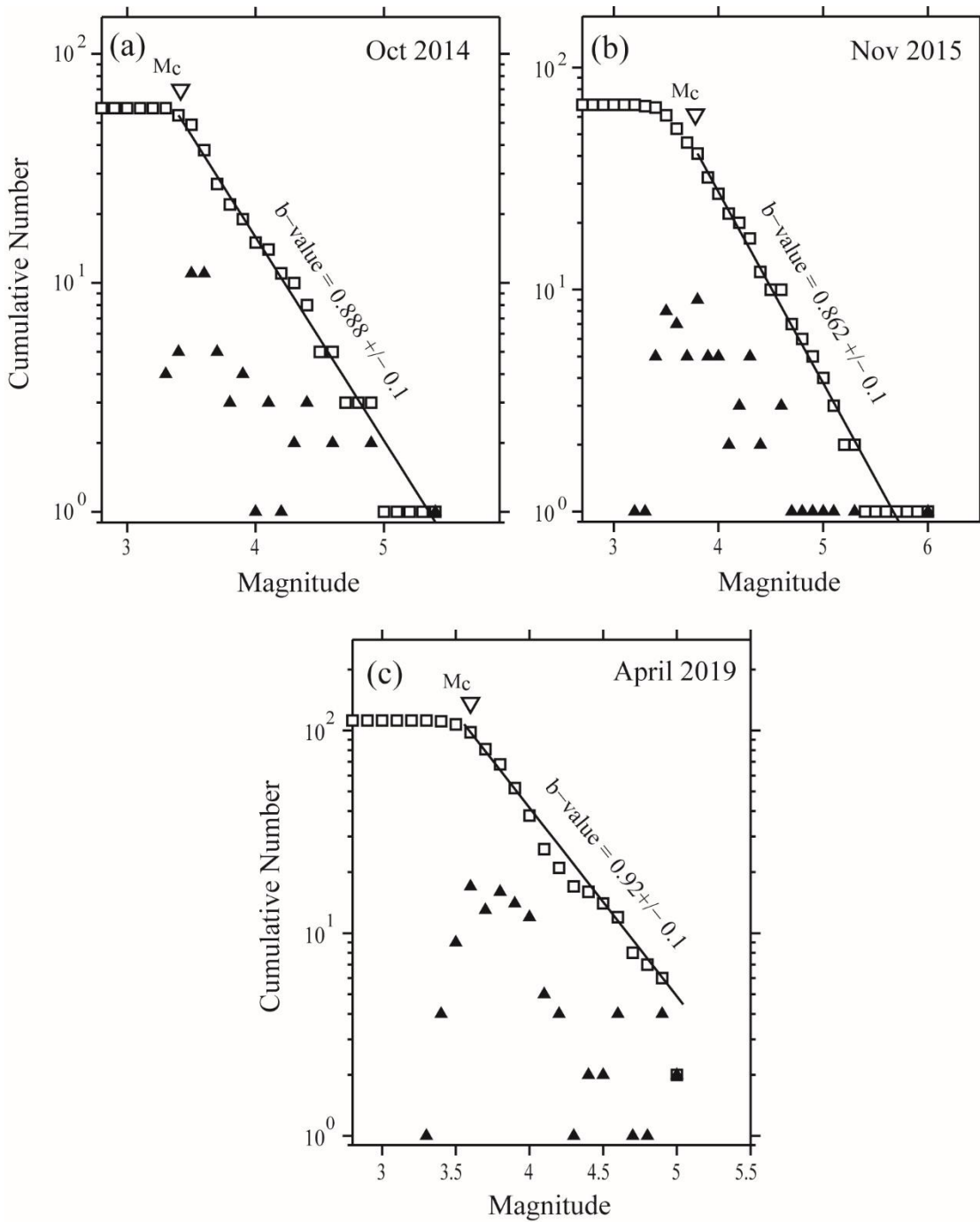


Figure S2. Cumulative magnitude-frequency and b -value of (a) October 2014, (b) November 2015, (c) April 2019 swarm away from volcanic arc. We estimated the b -value using maximum likelihood method using Zmap software. For calculating b -value distribution for the earthquake swarm we have chosen the maximum curvature fit of magnitude of completeness value (M_c). Squares and triangles represent cumulative number of earthquakes and first derivatives of the data to determine magnitude of completeness, respectively.